The Journal of Experimental Biology 201, 1871–1883 (1998)
Printed in Great Britain © The Company of Biologists Limited 1998
JEB1139

ONTOGENETIC SCALING OF HYDROSTATIC SKELETONS: GEOMETRIC, STATIC STRESS AND DYNAMIC STRESS SCALING OF THE EARTHWORM *LUMBRICUS TERRESTRIS*

KIM J. QUILLIN

Department of Integrative Biology, University of California, Berkeley, CA 94720-3140, USA

e-mail: quillin@socrates.berkeley.edu

Accepted 23 March; published on WWW 21 May 1998

Summary

Soft-bodied organisms with hydrostatic skeletons range enormously in body size, both during the growth of individuals and in the comparison of species. Therefore, body size is an important consideration in an examination of the mechanical function of hydrostatic skeletons. The scaling of hydrostatic skeletons cannot be inferred from existing studies of the lever-like skeletons of vertebrates and arthropods because the two skeleton types function by different mechanisms. Hydrostats are constructed of an extensible body wall in tension surrounding a fluid or deformable tissue under compression. It is the pressurized internal fluid (rather than the rigid levers of vertebrates and arthropods) that enables the maintenance of posture, antagonism of muscles and transfer of muscle forces to the environment. The objectives of the present study were (1) to define the geometric, static stress and dynamic stress similarity scaling hypotheses for hydrostatic skeletons on the basis of their generalized form and function, and (2) to apply these similarity hypotheses in a study of the ontogenetic scaling of earthworms, *Lumbricus terrestris*, to determine which parameters of skeletal function are conserved or changed as a function of body mass during growth (from 0.01 to 8 g). Morphometric measurements on anesthetized earthworms revealed that the earthworms grew isometrically; the external proportions and number of segments were constant as a function of body size. Calculations of static stresses (forces per cross-sectional area in the body wall) during rest and dynamic stresses during peristaltic crawling (calculated from measurements of internal pressure and body wall geometry) revealed that the earthworms also maintained static and dynamic stress similarity, despite a slight increase in body wall thickness in segment 50 (but not in segment 15). In summary, the hydrostatic skeletons of earthworms differ fundamentally from the rigid, lever-like skeletons of their terrestrial counterparts in their ability to grow isometrically while maintaining similarity in both static and dynamic stresses.

Key words: biomechanics, scaling, hydrostatic skeleton, earthworm, *Lumbricus terrestris*, ontogeny, size.

Introduction

Body size influences almost every aspect of the biology of an organism, from its physiology and ecology to the mechanical functioning of its skeleton (reviewed in Gould, 1966; Currey, 1970; Alexander, 1971; Pedley, 1977; McMahon, 1973, 1975; McMahon and Bonner, 1983; Peters, 1983; Calder, 1984; Schmidt-Nielsen, 1984). Studies on the scaling of skeletons have concentrated on vertebrates, arthropods and trees whose rigid bones, exoskeletons and trunks, respectively, are loaded as beams and columns by their own body weight. Other studies have examined the scaling of structures loaded in pure tension (e.g. fruit stems and kelp stipes; Peterson *et al.* 1982; Johnson and Koehl, 1994). While these studies have established a foundation of useful scaling principles, they are not directly applicable to the problem of how hydrostatic skeletons scale.

Soft-bodied organisms with hydrostatic skeletons are abundant and diverse. Body mass differs by at least 13 orders of magnitude from giant squid (*Architeuthis* sp., 20 m long including tentacles) to minute nematode worms (less than 1 mm length) (Ruppert and Barnes, 1995). Body size also increases by orders of magnitude during the growth of many soft-bodied organisms, for example by four orders of magnitude in body mass in the earthworm *Lumbricus terrestris*. Clearly, size is an important variable for soft-bodied organisms, but what effect does body size have on the biomechanical functions of hydrostatic skeletons?

The hydrostatic skeletons of most soft-bodied organisms are constructed from an extensible body wall in tension surrounding a fluid or deformable tissue under compression (Chapman, 1958; Wainwright, 1988). The fluid under compression becomes pressurized, and it is this pressure (rather than the rigid levers of vertebrates and arthropods) that enables stiffening of the organism, antagonism of muscles and transfer of muscle forces to the environment (e.g. Chapman, 1958; Currey, 1970; Trueman, 1975). Hydrostatic skeletons may encompass whole organisms, either for an entire lifetime

(e.g. earthworms) or for one life-history stage (e.g. caterpillars), or alternatively may occur in just parts or appendages of an organism (e.g. tongues in vertebrates and tube feet in echinoderms). Hydrostatic appendages whose requisite incompressible fluid is contained within deformable muscle cells are called muscular hydrostats (e.g. elephant trunks and squid tentacles; Kier and Smith, 1985). In contrast, hydrostatic skeletons describe a body cavity filled with sea water, blood, coelomic fluid and/or deformable organ tissues (e.g. sea anemones, roundworms and earthworms; see Kier, 1992).

Objectives

How does a soft-bodied organism grow by orders of magnitude in body size yet maintain the biomechanical functions of its hydrostatic skeleton? The objectives of the present study were (1) to generate the geometric, static stress and dynamic stress similarity scaling hypotheses for hydrostatic skeletons on the basis of their form and function, and (2) to apply these similarity hypotheses to the ontogeny of the earthworm *Lumbricus terrestris* to determine which aspects of skeletal function are conserved or altered as a function of size during growth.

Scaling hypotheses

Whether a particular functional aspect of a skeleton is conserved or altered in relation to body mass is typically expressed in terms of a scaling hypothesis. Some hypotheses are based on form (‘geometric similarity’) whereas others are based on function (e.g. ‘stress similarity’). The functional similarity hypotheses have been defined previously in terms of the mechanism of mechanical function of lever-like skeletons. Since hydrostatic skeletons function by a qualitatively different mechanism from lever-like skeletons, both the predictions of the similarity hypotheses and their relationships to one another must be derived anew.

Geometric similarity

If two organisms are geometrically similar, or isometric, then linear dimensions are proportional to volume raised to the one-third power. Linear dimensions scale as $(\text{body mass})^{1/3}$ because mass is proportional to volume which is proportional to the cube of length, when body density is constant (e.g. Thompson, 1917; Alexander, 1971; Schmidt-Nielsen, 1984; Fig. 1). The exponential relationship between linear dimensions and body mass can be expressed by the function $y=am_b^b$ (Huxley, 1932), where m_b is body mass, y is a linear dimension, a is a constant and b is the exponent (1/3 in the case of geometric similarity). If the exponent is significantly different from 1/3, scaling is said to be allometric.

Most hydrostatic skeletons are cylindrical in shape, having an approximately round or elliptical cross section and an easily identifiable longitudinal axis (Wainwright, 1988). Therefore, the most important linear dimensions are length (L), diameter (d) and body wall thickness (t), all of which scale as $m_b^{1/3}$ in geometrically similar organisms in comparable postures, such as resting posture. If the cylindrical body of a hydrostat is divided into segments (as in annelids), then the number and linear dimensions of segments scale as m_b^0 and $m_b^{1/3}$, respectively, in geometrically similar organisms.

Static stress similarity

Static stress is the force (F) per cross-sectional area (A) of a skeletal element bearing the force when an organism is standing still (Thompson, 1917; Hill, 1950; McMahon, 1975). Static stress similarity occurs when static stress is constant as a function of body mass (i.e. stress $\propto m_b^0$). The loading of beam-like skeletons by body weight precludes the possibility that they are both geometrically and statically stress similar. Weight is proportional to the cube of the linear dimension, while the cross-sectional area of a skeletal element is proportional only to the square of the linear dimension. Therefore, static stress in a self-loaded beam can only remain constant as a function of body size if diameter increases at a greater rate than length (e.g. McMahon, 1975; Fig. 1). Bending beams must scale allometrically, not geometrically, to maintain static stress similarity.

The major source of static load on the body wall of a hydrostatic skeleton is internal pressure (P). Pressure can be generated by the contraction of muscles in the body wall surrounding the incompressible fluid and/or by mechanisms such as ciliary pumps (e.g. in sea anemones; Batham and Pantin, 1950), osmotic pressure (e.g. notochords; Adams *et al.* 1990) and gravitational pressure (the gradient of pressure produced in a static fluid by its own weight; e.g. Ellers and Telford, 1992). The magnitude of tensile stress in the body wall of a cylindrical hydrostatic skeleton is given by:

$$\sigma_c = \frac{Pr}{t} \quad \text{and} \quad \sigma_l = \frac{Pr}{2t}\ , \tag{1}$$

(Fig. 2A; Chapman, 1950), where σ_c is the circumferential tensile stress, σ_l is the longitudinal tensile stress, P is the internal pressure, r is the radius and t is the body wall thickness. The stress is distributed uniformly over the thickness of the wall provided that the wall is very thin (generally indicated by a ratio r/t that is greater than 10; Gere and Timoshenko, 1984). The thicker the wall relative to the radius, the more important shear stress becomes because of the differential in tensile stress between the outside and the inside of the wall. The maximum shear stress (τ_{max}) in the body wall is given by:

$$\tau_{max} = \frac{Pr}{2t} + \frac{P}{2}\ , \tag{2}$$

where the last term is generally disregarded when the ratio r/t is high (Gere and Timoshenko, 1984). Since shear stress is directly proportional to tensile stress for a given cylinder, and since maximum tensile stress is generally of greater magnitude than maximum shear stress, tensile stress will be the focus of the remainder of this study.

Unlike the case for rigid skeletons, static stress similarity is

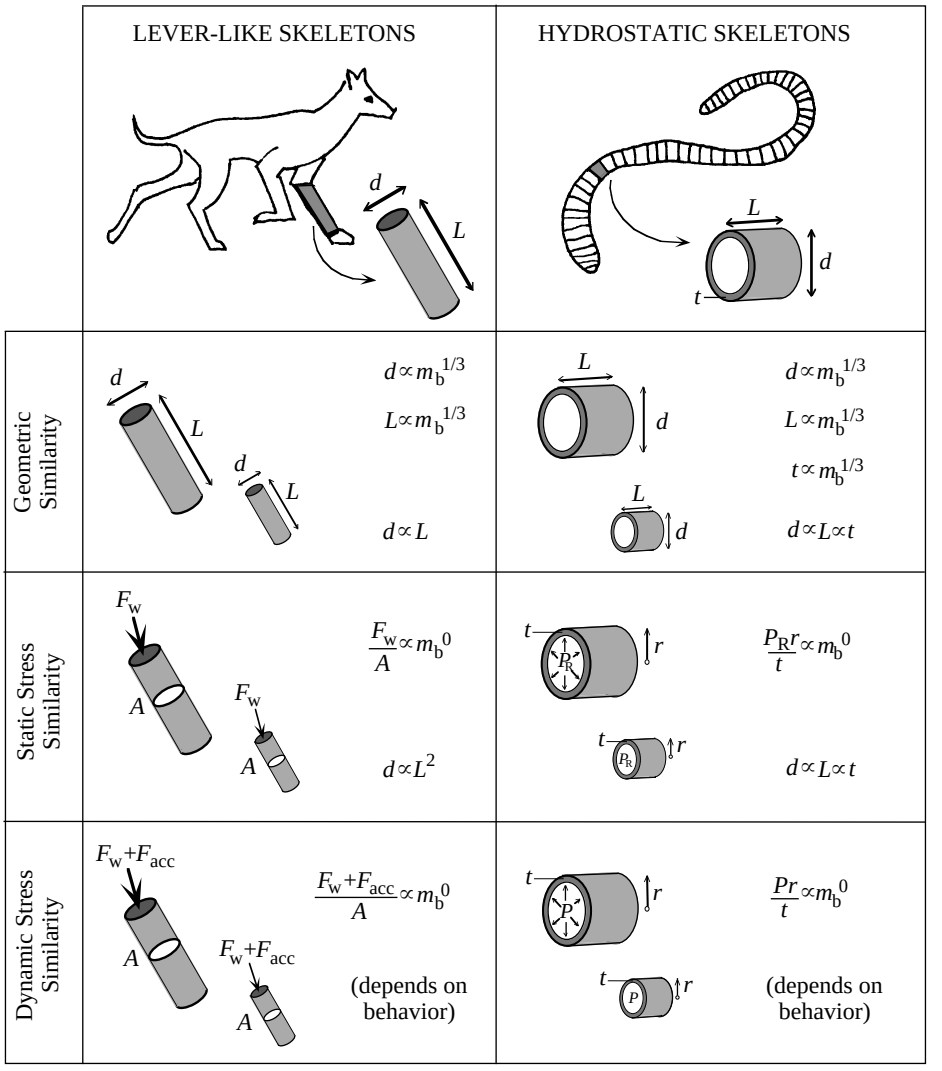

Fig. 1. Schematic comparison and contrast of the similarity hypotheses for organisms with lever-like skeletons *versus* organisms with hydrostatic skeletons. See Introduction for further details. d, diameter; L, length, t, body wall thickness; m_b, body mass, F_w, force due to body weight; A, cross-sectional area of a skeletal element bearing the load; P_R, internal pressure during rest; P, internal pressure; r, radius; F_{acc}, ground reaction force.

not excluded by geometric similarity in hydrostatic skeletons, and *vice versa*; hydrostats that are geometrically similar (and therefore possess the same r/t ratio) may or may not show static stress similarity depending on the magnitude of internal pressure. Likewise, hydrostats that are *not* geometrically similar may or may not show static stress similarity depending on the magnitude of internal pressure.

The scaling of static stress depends on the source of internal pressure in animals at rest. Many animals, such as the marine polychaete *Arenicola marina*, maintain muscle tension during rest to stiffen the body and maintain a resting posture (Chapman and Newell, 1947; Trueman, 1966), much as we maintain tension in our leg muscles to keep ourselves from falling down when we are standing still. In such cases, where muscle tension is the only source of internal pressure (P_m), geometrically similar hydrostats will be stress similar as long as muscle stress (σ_m) does not vary with body size ($\sigma_m \propto m_b^0$). The internal pressure resulting from muscle tension is given by:

$$P_m = (\sigma_m A_m) A_i^{-1}, \quad (3)$$

where both the cross-sectional area of the muscle (A_m) and the projected inside area of the hydrostat (A_i; Fig. 2B) scale as $m_b^{2/3}$ such that:

$$P_m \propto m_b^{0+2/3-2/3}; \quad (4)$$

hence

$$P_m \propto m_b^0. \quad (5)$$

Thus, geometrically similar organisms with internal pressure derived from muscle tension should show static stress similarity unless the muscle properties or the behavior of the organisms change with body size. Note that body wall stress will necessarily equal muscle stress only when the body wall thickness is composed entirely of one muscle layer.

If the total internal pressure (P) in a hydrostat is derived from sources other than or in addition to P_m, then the scaling of these sources must also be considered. Gravitational pressure (P_g) is insignificant in most aquatic soft-bodied organisms because the pressure gradient outside the body wall due to the weight of the water column is the same as the pressure gradient within (Ellers and Telford, 1992). Gravitational pressure may, however, be an important variable

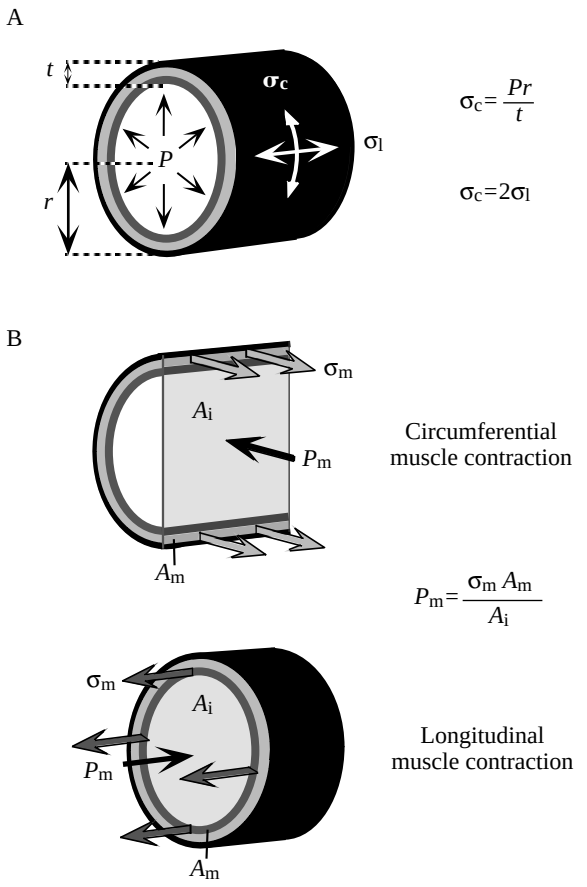

Fig. 2. Simplified diagram of an earthworm-like hydrostatic skeleton composed of a body wall in tension surrounding a fluid in compression. The body wall is composed of a layer of longitudinal muscle (dark gray), a layer of circumferential muscle (light gray) and a layer of epidermis and cuticle (black). (A) The circumferential stress (σ_c) in a cylindrical hydrostatic skeleton of uniform radius (r) and thickness (t) is the product of internal pressure (P) and the ratio of radius to thickness. The magnitude of longitudinal stress (σ_l) is half the magnitude of circumferential stress. (B) The magnitude of internal pressure resulting from muscle tension (P_m) for both circumferential and longitudinal muscle contractions is determined by the muscle stress (σ_m), the cross-sectional area of muscle (A_m) and the projected inside area of the hydrostat (A_i).

in some terrestrial hydrostats. Gravitational pressure at a given point in an organism is given by:

$$P_g = \rho \boldsymbol{g} z , \quad (6)$$

where ρ is the density of the fluid and tissue, $\boldsymbol{g}$ is the acceleration due to gravity, and z is the vertical distance from the upper surface of the organism to that point (Ellers and Telford, 1992). A larger organism will have a greater maximum P_g than a geometrically similar smaller organism because of its greater vertical linear dimension (z), such that $P_g \propto m_b^{1/3}$ when body density is constant (unless the larger organism is sufficiently flexible to flatten slightly under its own weight). Thus, geometrically similar organisms for which P_g is an important source of pressure may not maintain static stress similarity.

Dynamic stress similarity

Animals experience dynamic stresses in their skeletons when they move. The dynamic strain similarity hypothesis of Rubin and Lanyon (1984; so-named because they calculated stresses from their measurements of bone strains) states that the maximum stress experienced by a skeletal element during vigorous locomotion is independent of body size and thus scales as m_b^0 (Fig. 1). Maximum stress during locomotion in legged animals is greater than resting stress owing to the addition of the ground reaction forces (F_{acc}) required to accelerate and decelerate the animal. The magnitude of ground reaction forces is dependent not only on the weight of the organism but also on the gait it uses. Therefore, the dynamic strain similarity hypothesis as applied to rigid skeletons is neither excluded nor predicted by geometric similarity alone; it must be measured while the organisms are in motion.

The maximum stress experienced by the body wall of a hydrostatic skeleton likewise depends on the organism's behavior. The internal pressures in most hydrostats fluctuate (Zuckerkandl, 1950), but tend to peak when muscle contractions peak (e.g. Chapman and Newell, 1947; Newell, 1950). However, hydrostats tend to be highly deformable, and the maximum r/t may not coincide with the pressure maximum. The maximum tensile stress occurs when and where the product of P and r/t is greatest (see equation 1). If the main source of internal pressure is muscle tension (P_m, which is likely to be the case) and if muscle properties do not vary with body size, then geometrically similar hydrostats should show dynamic stress similarity as long as behavior does not change during growth. Thus, internal pressure and body wall geometry must be measured in living hydrostats in order to test hypotheses of dynamic stress similarity.

Application of scaling hypotheses to Lumbricus terrestris

The first objective of the present study was to generate predictions for the geometric, static stress and dynamic stress scaling hypotheses for hydrostatic skeletons on the basis of their form and function. Given the formulated predictions, the next objective was to apply the similarity hypotheses to the ontogeny of the earthworm *Lumbricus terrestris* to determine which aspects of skeletal function are conserved or altered as a function of size during growth. *L. terrestris* was chosen as the experimental system because of its abundance, ease of study in the laboratory, and the availability of a large ontogenetic size range. Its segmented skeleton is composed of a body wall (cuticle, epithelium, two layers of muscle and connective tissue) surrounding coelomic fluid and deformable organ tissues. The volume of coelomic fluid within each segment is constant (Newell, 1950). Thus, when the circumferential muscles of a segment contract, the segment becomes long and slim as the passive longitudinal muscles are stretched. When the longitudinal muscles contract, the segment becomes short and wide and the circumferential muscles are stretched (Seymour, 1969). Alternating waves of circumferential and longitudinal muscle contractions travel posteriorly along the body, enabling

forward progression by peristalsis (e.g. Gray and Lissmann, 1938).

The experimental objectives of the present study were (1) to measure the resting geometry of the skeletons of earthworms as a function of size, (2) to measure internal pressures in resting earthworms in order to calculate the scaling of static tensile stresses in the body wall, and (3) to measure dynamic internal pressures in locomoting earthworms in order to calculate the scaling of dynamic tensile stresses in the body wall. The present study focuses on the earthworms during their most observed and understood activity – surface crawling – although peristalsis is also used by this species to burrow. Whereas most earthworm species are either geophagous (earth-eaters) or surface feeders, *Lumbricus terrestris* is both; as its common name 'night crawler' suggests, it feeds on the surface at night, drawing leaves and other organic materials into its semi-permanent burrows and digesting them within (Darwin, 1881; Arthur, 1965; Satchell, 1967). Thus, surface crawling is used as a pragmatic first assessment of dynamic stresses in the body wall.

Materials and methods

Experimental animals

Earthworms (*Lumbricus terrestris* L.) ranging in size from 0.3 to 8.0 g were obtained from Idaho (Loch Lomond Bait, San Rafel, CA, USA) and maintained at 6 °C in Magic Worm Ranches using Magic Worm Bedding and Magic Worm Food (Magic Products Inc., Amherst Junction, WI, USA). I supplemented this size range with juveniles (0.01–0.3 g) collected from an outdoor enclosure in Berkeley, CA, USA, in which I maintained *L. terrestris* from Canada (Berkeley Bait, Berkeley, CA, USA). Fig. 3 summarizes the size ranges used for each of the scaling variables examined.

Although earthworm segments are similar along the length of the body, some regionalization does occur. I chose two relatively dissimilar segments for comparison of diameter, body wall thickness, internal pressure and stress to assess the effects, if any, of this regionalization on the function and scaling of the hydrostatic skeleton. Segment 15 lies in the widest region of the worm near the anterior end, where segments are relatively long and wide and contain specialized digestive and reproductive organs. Segment 50, by contrast, lies in the relatively homogeneous midregion of the worm, where segments are narrower and shorter and are occupied primarily by the intestine (Fig. 4).

Pressure measurement

I made continuous measurements of internal pressure using a low-volume gauge pressure transducer (PX170, Omega Engineering, Stamford, CT, USA) designed to read pressures up to 7 kPa. I connected the transducer to a piece of water-filled flexible polyethylene tubing attached to a terminal cannula constructed from a 27 gauge hypodermic needle. The transducer was calibrated before each series of measurements by inserting the needle through the wall of a 2 cm vertical Nalgene tube that was open at the top. The tube height was raised so that the meniscus of the water level increased in height at 1 cm intervals with respect to the center of the transducer. The data were collected at 50 scans s^{-1} by LabVIEW software (version 3.0.1; National Instruments, Austin, TX, USA) on a Gateway 2000 computer.

Prior to insertion of the cannula, the earthworms were calmed by placement in dilute ethanol (1–5 % in spring water) for 20–40 min (response time to the anesthetic varied). After this procedure, worms did not thrash when handled but did exhibit typical locomotory peristalsis as observed in earthworms without a cannula inserted. I then placed the earthworms into a tray of fresh water 1 cm deep (meniscus level adjusted to the height of the center of the pressure transducer) rather than in air to keep the needle-tip submerged between measurements and to keep the tubing still while the worm crawled 'in place' in the water, avoiding pressure artifacts due to movement of the apparatus. I inserted the needle laterally into the coelom of each worm, just under the body wall in segments 15 and 50 or the adjacent segments (pressure among adjacent segments did not differ measurably).

The following variables were measured from the pressure records (to the nearest 10 Pa; Fig. 5): (1) maximum pressures during circumferential muscle contractions ($P_{C.M.}$), (2) maximum pressures during longitudinal muscle contractions ($P_{L.M.}$) and (3) resting pressures (P_R). The dynamic pressure measurements were averaged over 10 cycles of peristalsis. Resting pressures were recorded as often as possible but only

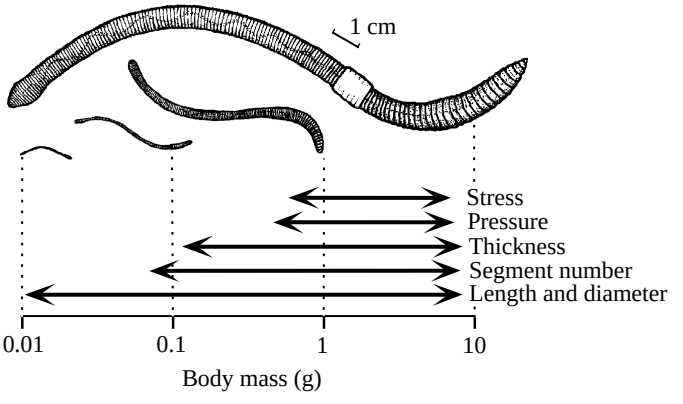

Fig. 3. Diagram illustrating the order-of-magnitude of size ranges (10^x) in body mass of *Lumbricus terrestris* used for each measurement: dynamic stress ($10^{1.1}$), internal pressure and static stress ($10^{1.2}$) and morphometrics ($10^{2.9}$), with segment number ($10^{2.1}$) and body wall thickness ($10^{1.7}$) measured in the upper end of the morphometric range. Earthworms are drawn to the same scale at order-of-magnitude intervals in body mass to illustrate the ontogenetic size range used.

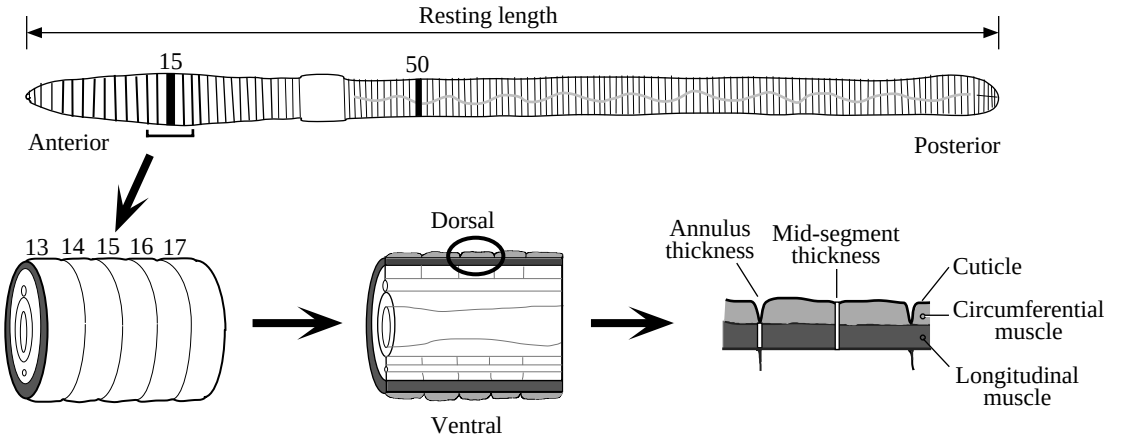

Fig. 4. Diagram illustrating the morphometric measurements made on *Lumbricus terrestris*. Resting length and the number of segments of the entire body, and resting lengths, lateral diameters and body wall thicknesses of segments 15 and 50 were measured on anesthetized earthworms as described in Materials and methods.

as they occurred between bouts of peristalsis (rather than in anesthetized or otherwise quiescent earthworms) to ensure that the cannula was not clogged. The number of pressure records available for each individual varied from zero to five; the mean resting pressure was calculated when more than one record was available.

Morphometrics

I anesthetized the earthworms to compare the dimensions of their highly extensible skeletons in comparable postures. First, I submerged the earthworms in spring water and slowly added drops of 50 % ethanol for 30–60 min. When the earthworms no longer responded to stimulation, I blotted them dry and measured the mass of the large and medium worms on a three-beam balance and the smallest worms on a Mettler balance (model AE 163) to two significant figures (i.e. to the nearest 0.1 g for the largest worms and to the nearest 0.0001 g for the smallest worms). I then counted the number of segments and measured body length with a ruler or digital calipers to the nearest 1 mm (or 0.1 mm in the case of very small worms) and the widths of segments 15 and 50 with calipers to the nearest 0.1 mm.

Body wall thickness was measured using frozen sections rather than standard histological sections to minimize shrinkage due to fixation. I rapidly froze anesthetized earthworms by sliding them off a straight edge into 95 % ethanol chilled to −78 °C using cubes of dry ice. Small worms froze immediately while large worms required 2–3 s; body dimensions did not change measurably during this period. I removed each frozen worm and cut it first transversely with a razor blade to remove two sections composed of segments 13–17 and 48–52, and then sagittally to produce two lateral halves of each section (Fig. 4). Images of these halves were captured using a high-resolution color video camera (Sony CCD-Iris SSC-C374) affixed to a Wild Heerbrugg dissecting microscope (model M5A). I used a RasterOps frame-grabber board to select individual video frames, and NIH Image software (Version 1.59) on a Power Macintosh 7100/80 to measure body wall thickness in the middle of segments 15 and 50 and at the annuli adjacent to these segments (Fig. 4).

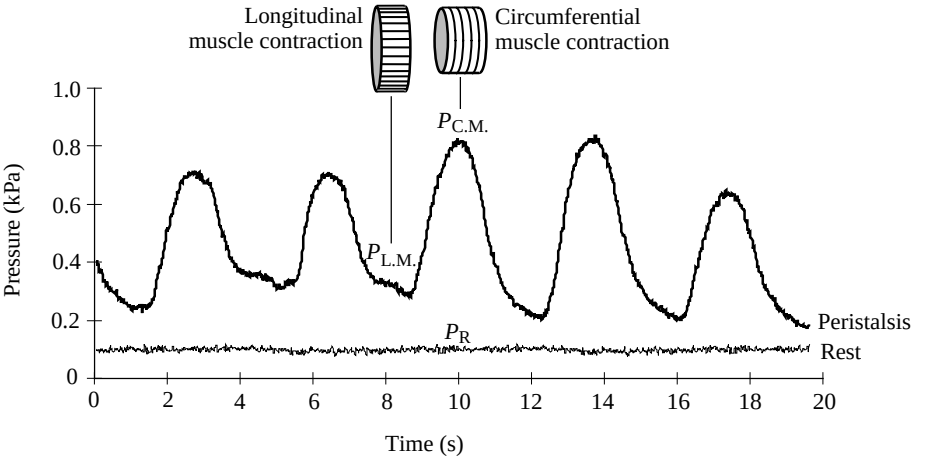

Fig. 5. Typical records of internal pressure during earthworm peristalsis (upper record) and during rest (lower record) showing the variables measured: maximum pressure during circumferential muscle contraction ($P_{C.M.}$), when the segment is long and narrow; maximum pressure during longitudinal muscle contraction ($P_{L.M.}$), when the segment is short and wide; and resting pressure (P_R), when the segment is relaxed.

Thickness was measured to the nearest 0.01 mm, and dorsal and ventral thicknesses were averaged. Segment length was measured to the nearest 0.01 mm. Circumferential muscle cross-sectional area was measured to the nearest 0.01 mm^2. The lower size limit of worms sectioned (Fig. 3) was determined by the lack of pigmentation in small worms, which rendered tissue layers difficult to distinguish.

Stress calculations

Static body wall tensile stresses were calculated from equation 1 using resting pressure and the resting radius and thickness values obtained from morphometric measurements of the same individuals. Since the body walls of earthworms do not have uniform thickness (Fig. 4), the annulus body wall thickness was used to calculate maximum resting longitudinal stress (because only the longitudinal muscles bear longitudinal loads). The mid-segment thickness was used to calculate resting circumferential stress (because both longitudinal and circumferential muscles bear circumferential loads and because circumferential stress is resisted by the muscular septae at each annulus).

Dynamic body wall tensile stresses were calculated using pressures obtained during maximum contractions of circumferential and longitudinal muscles and using radius and thickness values calculated from the resting dimensions of the segments and the maximum shape changes observed in the segments during peristalsis. I video-taped the shape changes of segments 15 and 50 of crawling earthworms through a Wild Heerbrugg dissecting microscope using a SONY CCD-Iris (SSC-C374) high-resolution color video camera and a time/date generator (Panasonic WJ-810). I used RasterOps Video Capture software on a Power Macintosh 7100/80 to grab video frames, and NIH Image software (Version 1.59) to measure the minimum and maximum length and lateral diameter of the segments to the nearest 0.1 mm. During longitudinal muscle contraction, the shapes of segments 15 and 50 did not differ from those of resting earthworms; therefore, the resting radius and thickness values were used for calculation of circumferential stress during longitudinal muscle contraction. During circumferential muscle contraction, the length of segments 15 and 50 of earthworms of all sizes increased by a factor of 1.6±0.2 (N=20), while the diameter decreased by a factor of 0.75±0.06 (means ± S.D., N=15) (K. J. Quillin, unpublished data). Using these values, I solved for the annulus thickness of the extended segments assuming that the volume of the body wall is constant.

Statistical analysis

The allometric relationships between each of the measured variables and body mass (g) were analyzed using linear regressions of log-transformed data, where the equation of the log-transformed allometric relationship is given by:

$$\log y = \log a + b\log m_b . \quad (7)$$

Ordinary regression analysis tends to underestimate the slope (b) owing to the incorrect assumption that there is no measurement error in the x variate, in this case body mass (Harvey and Pagel, 1991). The degree of underestimation of the slope may, however, be corrected using the reliability ratio (κ_{xx}) as described by Fuller (1987):

$$\beta = b(\kappa_{xx})^{-1}, \quad (8)$$

where b is the attenuated slope as calculated by ordinary regression analysis and β is the corrected slope. For continuous variables such as body mass, the reliability ratio (κ_{xx}) is the correlation coefficient between two determinations of the same characteristic. I measured the body mass of 10 individuals on separate days (the first day they were unanesthetized, a week later they were anesthetized). I then plotted the body mass from the first day against the body mass from the second day and calculated the correlation coefficient r (r=κ_{xx}) and from this calculated each corrected slope β. The reliability ratio κ_{xx} calculated for body mass was 0.995; therefore, all regression slopes plotted as a function of body mass were increased by a factor of 1.005.

Student's t distribution was used to test slopes where the null hypothesis was β=0 or β=1/3. Analysis of covariance (ANCOVA) tests of homogeneity of slopes were performed to test whether observed slopes were significantly different from each other (Sokal and Rohlf, 1969). Independent-sample and paired-sample t-tests were performed to compare internal pressures in segment 15 *versus* segment 50. All statistical analyses were performed using Systat for Windows, version 5. Values are given as means ± standard deviations (S.D.).

Results

Geometric similarity

The external dimensions of the earthworms increased isometrically. Segment number (n) varied among individuals (147±13, N=111), but did not increase with body mass m_b over the two orders of magnitude size range investigated ($n \propto m_b^{0.01}$; the slope was not significantly different from zero, P>0.10; Fig. 6), indicating that the earthworms grew by enlarging each

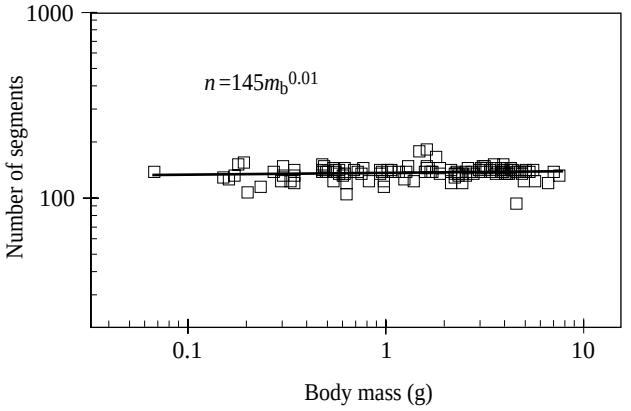

Fig. 6. Segment number n as a function of body mass m_b on logarithmic coordinates. The slope of the linear regression is not significantly different from zero (P>0.10; N=111; r^2=0.01).

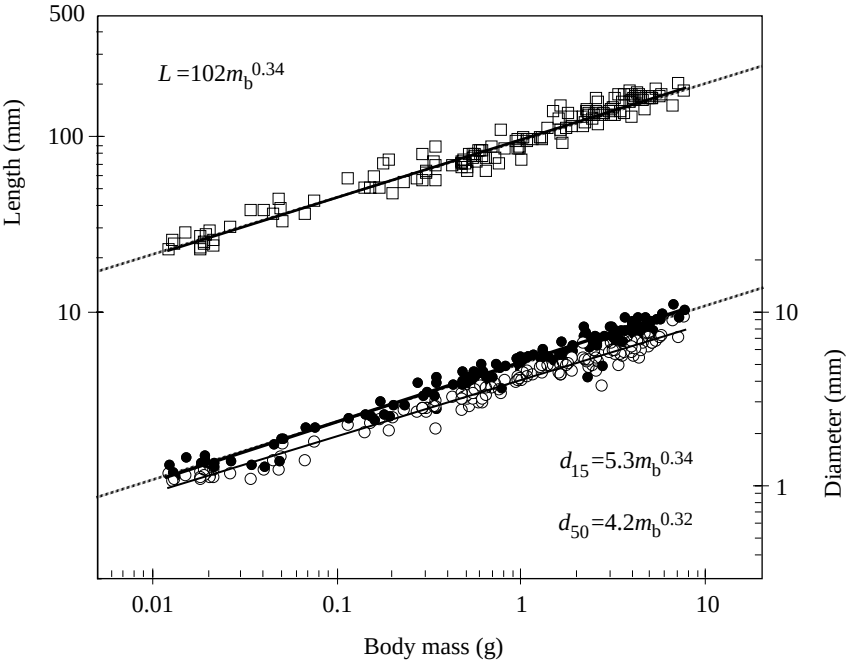

Fig. 7. Resting body length L (□; N=164; r^2=0.99; P<0.001 compared with a slope of zero) and lateral diameter of segments 15, d_{15} (●; N=160; r^2=0.98; P<0.001), and 50, d_{50} (○; N=162; r^2=0.98; P<0.001), as a function of body mass m_b on logarithmic coordinates. None of the slopes of the linear regressions is significantly different from 0.33 (broken lines), the slope predicted by isometry (P>0.10 for length; P=0.061 for both diameters).

segment rather than by adding segments. Furthermore, the resting lengths L_s of segment 15 (L_s=0.011$m_b^{0.32}$; r^2=0.82, N=19) and segment 50 (L_s=0.007$m_b^{0.34}$; r^2=0.79, N=19) increased at the rate predicted by geometric similarity (the slopes were significantly different from zero, P<0.001, but not significantly different from 0.33, P>0.10). The resting diameters (d_{15}, d_{50}) of both segments also increased as predicted by geometric similarity ($d_{15}\propto m_b^{0.34}$, $d_{50}\propto m_b^{0.32}$; P=0.061 for both compared with a slope of 0.33, P<0.001 for both compared with a slope of zero; Fig. 7), indicating that earthworms increased their segment dimensions isometrically. The resting length of the entire body increased with body mass at the same rate as predicted by geometric similarity ($L\propto m_b^{0.34}$; P>0.10 compared with a slope of 0.33, P<0.001 compared with a slope of zero, N=164; Fig. 7). The mean length/diameter ratio over the entire size range was 21.8±4.0 (N=135).

Body wall thickness increased isometrically in segment 15, but allometrically in segment 50 (Fig. 8). The mid-segment and annulus thicknesses of segment 15 increased isometrically as $m_b^{0.37}$ and $m_b^{0.38}$ respectively (P>0.10 compared with a slope of 0.33, P<0.001 compared with a slope of zero). However, the mid-segment and annulus thicknesses of segment 50 grew allometrically as $m_b^{0.42}$ (P=0.004 compared with a slope of 0.33) and $m_b^{0.45}$ (P<0.001), respectively. The allometric increase in body wall thickness reflects an allometric increase in the cross-sectional area of the muscles; the mid-sagittal cross-sectional areas of circumferential muscle in the body wall of segments 15 and 50 increased as $m_b^{0.90}$ (r^2=0.90, N=20) and $m_b^{0.91}$ (r^2=0.81, N=20), respectively, which were both greater than the slope 0.67 predicted by isometry (P=0.006 for segment 15, P=0.037 for segment 50).

Despite allometry in body wall thickness, the longitudinal and circumferential muscles maintained their relative proportions during growth (Fig. 8). The slopes of the mid-segment body wall thicknesses (a measure of circumferential muscle plus longitudinal muscle plus epidermis and cuticle thickness) were not significanly different (P>0.10) from the slopes of the annulus body wall thicknesses (a measure of longitudinal muscle plus epidermis and cuticle thickness; see Fig. 4).

Static stress similarity

Resting pressures P_R differed greatly from individual to individual (115±45 Pa; N=19), but scaled independently of body mass over the one-order-of-magnitude range in body mass observed ($P_R\propto m_b^{-0.003}$; P>0.10 compared with a slope of zero; Fig. 9). Resting pressures in segments 15 and 50 were not significantly different (independent t-test, P>0.10), so these data were pooled for the calculation of stress.

Static tensile stress in the body wall of the earthworms was constant as a function of body mass. The static circumferential stress σ_c in the mid-segment body wall scaled as $m_b^{-0.07}$ and $m_b^{-0.09}$ in segments 15 and 50, respectively, neither of which was different from a slope of zero (P>0.10; Fig. 10). The static longitudinal stress σ_l in the longitudinal muscle layer scaled as $m_b^{0.10}$ and $m_b^{0.07}$ in segments 15 and 50, respectively, neither of which was significantly different from a slope of zero (P>0.10; Fig. 9). The mean static circumferential stresses were 830±330 Pa and 710±300 Pa (N=19) for segments 15 and 50, respectively. The mean static longitudinal stresses were 64±15 Pa and 55±13 Pa (N=19) for segments 15 and 50, respectively.

Dynamic stress similarity

Since the mean internal pressures during maximum circumferential muscle contraction $P_{C.M.}$ in segments 15

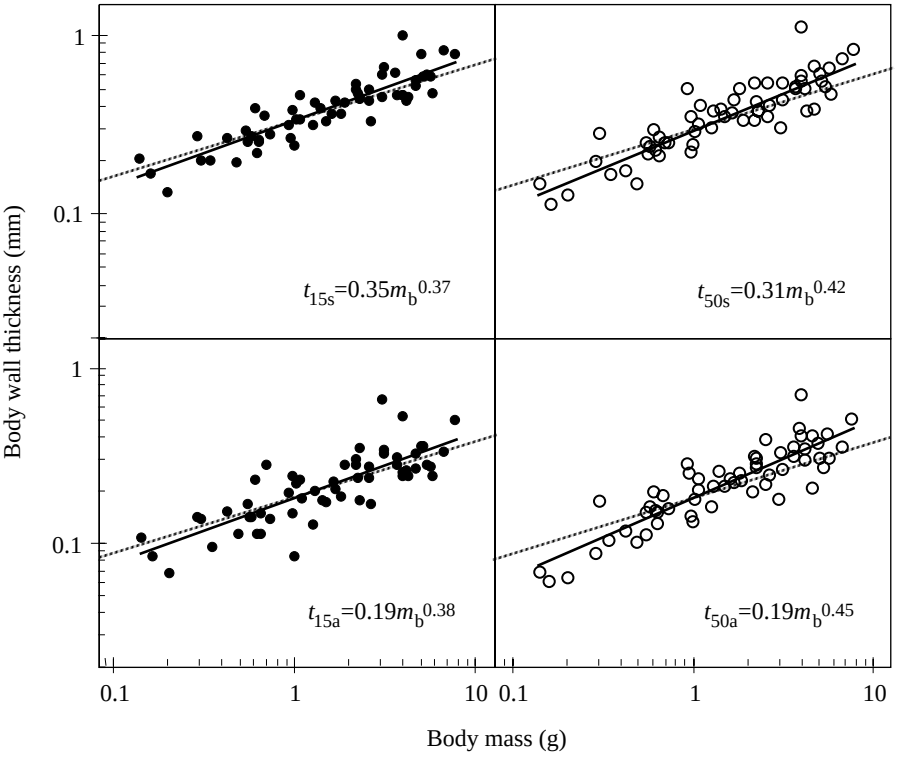

Fig. 8. Body wall thickness as a function of body mass m_b on logarithmic coordinates (N=59). The slopes of the linear regressions for mid-segment thickness (t_{15s}; r^2=0.80) and annulus thickness (t_{15a}; r^2=0.65) for segment 15 (●) are significantly different from a slope of zero (P<0.001), but not significantly different from 0.33, the slope predicted by isometry (broken lines; P>0.10). The slopes of the linear regressions for mid-segment thickness (t_{50s}; r^2=0.78) and annulus thickness (t_{50a}; r^2=0.79) for segment 50 (○) are significantly greater than 0.33 (broken lines; P=0.004 and P<0.001, respectively).

(580±220 Pa) and 50 (670±300 Pa) were not significantly different (P>0.10), these data were pooled for the calculation of stress. However, the internal pressures during maximum longitudinal muscle contraction $P_{L.M.}$ in segments 15 (300±220 Pa) and 50 (550±260 Pa) were significantly different (P=0.018), and so were not pooled for the calculation of stress.

Maximum dynamic stresses in the body wall during peristalsis were independent of body mass (Fig. 10). The mean maximum pressure during circumferential muscle contraction $P_{C.M.}$ scaled as $m_b^{0.04}$ (Fig. 9), and the resulting maximum longitudinal stress σ_l in the body wall scaled as $m_b^{0.01}$ and $m_b^{-0.19}$ in segments 15 and 50, respectively (Fig. 10). The mean maximum pressure during longitudinal muscle contraction $P_{L.M.}$ scaled as $m_b^{-0.05}$ (Fig. 9), and the resulting maximum circumferential stress σ_c in the body wall scaled as $m_b^{-0.07}$ and $m_b^{-0.09}$ in segments 15 and 50, respectively. None of the regression slopes was significantly different from zero (P>0.10), indicating that earthworms show dynamic stress similarity in peristaltic crawling as they grow. The amplitude of stress fluctuation during peristalsis was higher in segment 15 than in segment 50 (P<0.001; Fig. 10), but the amplitude did not change significantly as a function of body mass (P>0.10).

In the resting earthworm, circumferential tensile stress was greater than longitudinal tensile stress (Fig. 10). In the crawling earthworm, however, longitudinal tensile stress

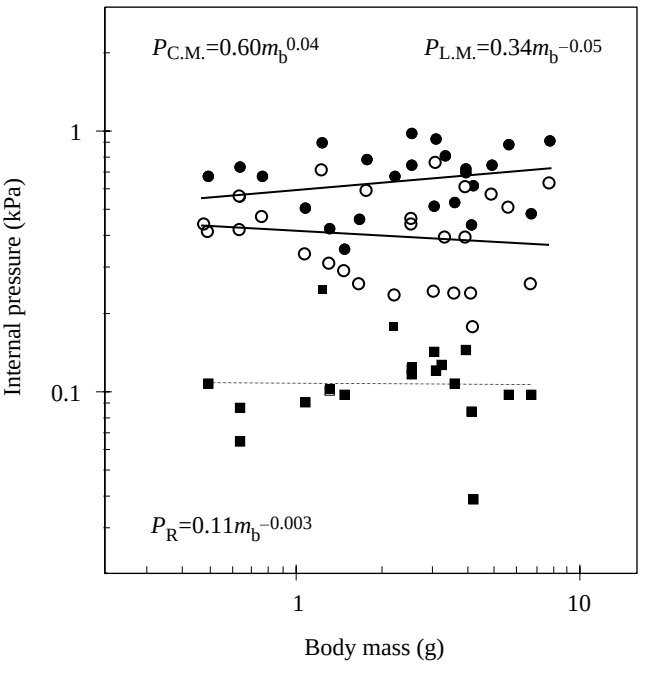

Fig. 9. Internal pressure as a function of body mass m_b on logarithmic coordinates. The slopes of the linear regressions for maximum internal pressure during circumferential muscle contraction ($P_{C.M}$ ●; N=26; r^2=0.01), maximum internal pressure during longitudinal muscle contraction ($P_{L.M.}$ ○; N=22; r^2=0.01), and rest (P_R ■; N=19; r^2=0.00003) are not significantly different from zero (P>0.10). $P_{C.M.}$ and P_R of segments 15 and 50 were not significantly different (P>0.10) and so were pooled. Values of $P_{L.M.}$ in segment 15 ($P_{L.M.15}$=0.34$m_b^{-0.05}$; r^2=0.01) were significantly lower (P<0.001) than those in segment 50 ($P_{L.M.50}$=0.44$m_b^{-0.002}$; r^2=0.00001) but are shown pooled here for clarity.

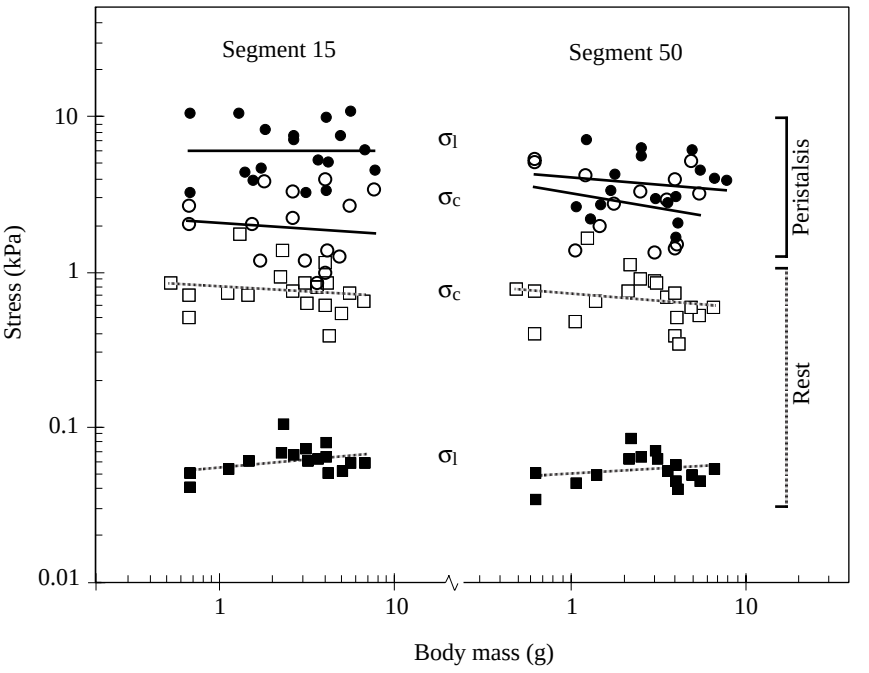

Fig. 10. Body wall stress as a function of body mass m_b on logarithmic coordinates. In segment 15, longitudinal stress σ_l in the body wall during maximum circumferential muscle contraction (●; $\sigma_l=6.1m_b^{0.01}$, N=19; r^2=0.001) was greater than circumferential stress σ_c during maximum longitudinal muscle contraction (○; $\sigma_c=2.1m_b^{-0.07}$, N=17; r^2=0.01) during surface peristalsis. Static circumferential stress (□; $\sigma_c=0.8m_b^{-0.07}$, N=19; r^2=0.02) was greater than static longitudinal stress (■; $\sigma_l=0.03m_b^{0.10}$, N=16; r^2=0.12). Likewise in segment 50, longitudinal stress in the body wall during maximum circumferential muscle contraction (●; $\sigma_l=4.1m_b^{-0.09}$, N=19; r^2=0.03) was greater than circumferential stress during maximum longitudinal muscle contraction (○; $\sigma_c=3.2m_b^{-0.19}$, N=14; r^2=0.07) during surface peristalsis. Static circumferential stress (□; $\sigma_c=0.7m_b^{-0.09}$, N=19; r^2=0.04) was greater than static longitudinal stress (■; $\sigma_l=0.03m_b^{0.07}$, N=16; r^2=0.05). None of the slopes of the linear regressions was significantly different from zero (P>0.10).

during circumferential muscle contraction was greater than circumferential tensile stress during longitudinal muscle contraction as a result of the higher pressures generated during circumferential muscle contraction (Fig. 9) and smaller cross-sectional area of the body wall experiencing longitudinal forces (Fig. 4).

The highest pressures recorded in the present study occurred during violent, whole-body contractions rather than during normal peristaltic crawling. Pressures reached 6.2 kPa in a 5.5 g earthworm and 4.3 kPa in a 1.8 g earthworm. The resulting circumferential stresses were calculated as 44 and 33 kPa, respectively.

Discussion

The earthworm *Lumbricus terrestris* grows isometrically while maintaining static and dynamic stress similarity. Unlike rigid skeletons, for which geometric similarity and static stress similarity are mutually exclusive hypotheses, hydrostatic skeletons can simultaneously maintain similarity in both form and this aspect of mechanical function as they grow.

Gravity and the scaling of hydrostatic skeleton function

The main source of loading on the skeleton of most terrestrial organisms with rigid skeletons is body weight. In earthworms, the main source of loading on the skeleton is internal pressure (generated by body wall muscles contracting against a constant volume of internal fluid). The pressure measurement apparatus used in the present study necessitated submerging the earthworms in a shallow bath of water to prevent air from entering the system and to prevent pressure artifacts due to the movement of the apparatus. Thus, gravitational pressure (P_g) was essentially eliminated as a source of total internal pressure. A horizontally oriented earthworm that is 1 mm in dorsoventral diameter should have a dorsoventral gradient in pressure that ranges from zero at the dorsal perimeter to a maximum P_g of 10 Pa at the ventral perimeter. An earthworm that is 10 mm in dorsoventral diameter should have a pressure gradient that ranges from zero to a maximum P_g of 100 Pa. These pressures lie within the variation in resting pressure measured in the present study (Fig. 9), and thus would not affect the resting pressure regression appreciably. Furthermore, the estimated gravitational pressures are considerably smaller than the pressures that occurred during peristalsis and therefore appear to be relatively unimportant. Vertically oriented earthworms (e.g. in vertical burrows) would not necessarily have higher gravitational pressures than horizontally oriented earthworms since muscular septae divide the coelom into constant-volume segments which prevent the transfer of pressure along the length of the body. Overall, the decoupling of body weight and skeletal function probably accounts to a great extent for the ability of a terrestrial hydrostatic skeleton to grow isometrically while maintaining stress similarity.

Lumbricus terrestris is generally considered to be a large earthworm compared with other temperate species (e.g. Arthur, 1965; Pierce, 1983), but several ‘giant’ species, measuring meters in length, can be found in the tropics (Stephenson, 1930). The upper limit to the size of hydrostatic skeletons is unclear, but some of the possible limitations to giant earthworms include (1) a decreased respiratory surface area due to the low surface-to-volume ratio compared with that of smaller earthworms, (2) an increased importance of gravitational pressure as a source of load on the body wall, (3) an increased frictional resistance to burrowing, and (4) the

exponential increase in the cost of tunnel construction with increasing body diameter (Gans, 1973). Present evidence suggests that larger earthworm species generally possess a higher length/diameter ratio and more segments than smaller earthworm species (Arthur, 1965; Piearce, 1983); this allometry may enable earthworms to reach the upper limit of body mass for terrestrial hydrostatic skeletons.

Scaling of segment shape

Segments are the constant-volume functional units of the skeletons of earthworms. Some species add segments during post-emergent growth (Evans, 1946; Piearce, 1983), but *Lumbricus terrestris* possesses the same number of segments throughout its lifetime (unless segments are lost as a result of predation; Evans, 1946). The number of segments and their dimensions are important for several reasons. In general, the greater the degree of segmentation of the skeleton, the greater the potential for localization of forces, pressures and shape changes in the skeleton and, hence, the greater the potential for complex motions (Clark, 1964). Furthermore, since the muscular septae between segments radially reinforce the cylindrical structure, the number of segments for a given body length may affect the resistance of the body to circumferential bulging and sagging (e.g. Seymour, 1970). A large number of septae per body length may also diminish the pressure gradient established along the length of an earthworm oriented vertically in its burrow.

The number and dimensions of the segments are also important in determining the velocity advantage of a hydrostatic skeleton. The velocity advantage is expressed by the ratio U_2/U_1, where U_1 is the rate of contraction of a muscle and U_2 is the maximum resulting velocity of an attached skeletal element (e.g. Alexander, 1983). In vertebrates and arthropods, the amplification of velocities is accomplished by rigid levers rotating about pivots. The velocity advantage of hydrostatic skeletons is determined by the simple geometric relationship between length and diameter in a constant-volume deformable cylinder (Fig. 11; Chapman, 1950; Kier and Smith, 1985). Both segments 15 and 50 have resting length/diameter ratios less than 1. This means, for example, that only a slight shortening of the longitudinal muscles is necessary for a large and rapid increase in diameter, enabling the earthworm to anchor quickly. Since the length and diameter of segments 15 and 50 did not differ significantly as a function of body mass, the segments of large and small worms appear to possess the same velocity advantage. Velocity advantage and mechanical advantage tend to be inversely related, but mechanical advantage has yet to be measured in hydrostatic skeletons.

The length/diameter ratio of an earthworm is not only important to the mechanical function of the skeleton, but also to the physiology of the organism. Gaseous exchange in earthworms occurs by diffusion across the skin (for a review, see Edwards and Bohlen, 1996), and the rate of water loss is also likely to be proportional to body surface area (Piearce, 1983). Since the surface area of *L. terrestris* decreases relative to its body mass during ontogeny (growth is isometric; thus, surface area $\propto m_b^{2/3}$), either larger earthworms have a lower respiratory rate and activity level than smaller earthworms or the decrease in relative surface area is compensated by other physiological variables such as the degree of vascularization of the body wall or the oxygen-carrying capacity of hemoglobin.

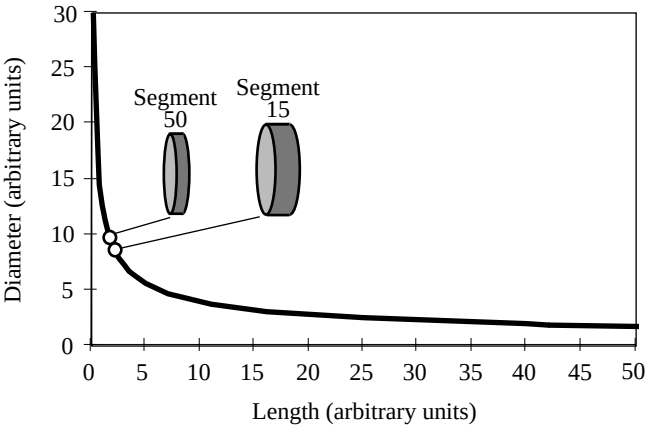

Fig. 11. Relationship between the diameter and length of a constant-volume cylinder in arbitrary units. Although segments 15 and 50 of the earthworm *Lumbricus terrestris* have different volumes, their resting dimensions are plotted on the same curve for comparison. Both segments have a resting diameter/length ratio greater than 1. Thus, only a small length change is required to cause a large change in diameter.

Whereas I observed isometric growth in *L. terrestris* ($L \propto d^{1.05}$), Piearce (1983) observed an increase in the length/diameter ratio as a function of body mass ($L \propto d^{1.28}$) in preserved specimens of the same species, such that larger worms were skinnier relative to their length than were smaller worms. All of the individuals observed by Piearce (1983) possessed a lower length/diameter ratio ($L/d \approx 18$) than I observed in the present study ($L/d \approx 22$). Preservation artifacts or interpopulational differences in diet and habitat are possible sources of this discrepancy.

Scaling of internal pressure

Neither resting pressure nor peak pressures during peristalsis changed as a function of body mass, and values were comparable to, but on average lower than, those reported for adult worms of the same species by Seymour (1969; mass range 4–6 g) and Newell (1950; mass range not provided). Since both body geometry and internal pressures were essentially independent of body mass in *L. terrestris*, I predict that the maximum force exerted on the environment by an earthworm per area of force application will be constant as a function of body mass ($F/A_f \propto m_b^0$), providing that muscle stress is constant. However, given the allometric increase in body wall thickness of segment 50, maximum internal pressures and thus the maximum force exerted by the mid-

region of large earthworms may be greater than that in small earthworms during burrowing. I am currently testing these alternative hypotheses.

One might expect internal pressure to peak during both circumferential and longitudinal muscle contractions, since these muscles are said to antagonize one another *via* internal pressure (e.g. Chapman, 1950). In the present study, internal pressure peaked during circumferential muscle contraction but decreased (sometimes nearly to resting pressure) during longitudinal muscle contraction (Fig. 5). Seymour (1969) hypothesized that the body wall, which is stiffened by the collagen-fiber-reinforced cuticle and subepidermal connective tissue, may act as a spring, storing potential energy upon circular muscle contraction which can be released to aid the longitudinal muscles in shortening upon the relaxation of the circumferential muscles. This spring-like behavior of segments may also be a simple byproduct of the dynamic shape changes of the constant-volume segments. Clark and Cowey (1958) established that a unit length of an open-ended cylinder bounded by crossed-helical collagen fibers contains the greatest volume when the angle between the fibers and the longitudinal axis of the cylinder is 54°44′ (see Fig. 1 in Clark and Cowey, 1958). The fiber angle of an adult earthworm cuticle is approximately 45° when the animals are at rest (Richards, 1974; Lepescheux, 1988). Since the volume of a segment is constant, the volume cannot decrease when the circumferential muscles contract (causing the segment to become longer and slimmer and the fiber angle to decrease), resulting in an increase in internal pressure. Likewise, the volume of a segment cannot increase when the longitudinal muscles contract (causing the segment to become short and wide and the fiber angle to increase), so the pressure decreases. It is not known how the fiber angle of the cuticle scales, nor how the material properties of the intact body wall scale (including the passive and active material properties of the muscle). Such information would help to determine the importance of elastic energy storage in explaining the observed patterns of segment shape change and internal pressure fluctuation.

In conclusion, soft-bodied organisms with hydrostatic skeletons are abundant and diverse and range in body mass over many orders of magnitude both within and among taxa. The present study used earthworms (*Lumbricus terrestris*) as an experimental system to begin an examination of how hydrostatic skeletons scale during ontogeny. Earthworms show geometric similarity and maintain static and dynamic stress similarity as they grow over several orders of magnitude in body mass. The hydrostatic skeletons of earthworms, therefore, differ fundamentally from the rigid lever-like skeletons of their terrestrial counterparts in their ability to grow isometrically while maintaining static stress similarity. Overall, the qualitatively distinct manner of mechanical function of hydrostatic skeletons and the relative unimportance of gravitational loads probably account to a great extent for the difference between the scaling of hydrostatic skeletons and terrestrial lever-like skeletons.

List of symbols

a	y-intercept of log-transformed allometric power-law function
A	cross-sectional area of a skeletal element bearing a force (m^2)
A_f	external area of application of force (m^2)
A_i	projected inside area of a hydrostat (m^2)
A_m	cross-sectional area of muscle (m^2)
b	exponent of allometric power-law function
d	diameter (m)
d_{15}	lateral diameter of segment 15 (m)
d_{50}	lateral diameter of segment 50 (m)
F	force (N)
F_{acc}	ground reaction force (N)
F_w	force due to the weight of the organism (N)
$\boldsymbol{g}$	gravitational acceleration ($m\,s^{-2}$)
L	resting body length (m)
L_s	resting segment length (m)
m_b	body mass (g)
n	number of segments
P	internal pressure ($N\,m^{-2}$)
$P_{C.M.}$	internal pressure during circumferential muscle contraction ($N\,m^{-2}$)
P_g	gravitational pressure ($N\,m^{-2}$)
$P_{L.M.}$	internal pressure during longitudinal muscle contraction ($N\,m^{-2}$)
P_m	internal pressure due to muscle tension ($N\,m^{-2}$)
P_R	internal pressure at rest ($N\,m^{-2}$)
r	radius (m)
t	body wall thickness (m)
t_{15a}	annulus body wall thickness of segment 15 (m)
t_{15s}	mid-segment body wall thickness of segment 15 (m)
t_{50a}	annulus body wall thickness of segment 50 (m)
t_{50s}	mid-segment body wall thickness of segment 50 (m)
U_1	rate of contraction of a muscle ($m\,s^{-1}$)
U_2	maximum velocity of a skeletal element ($m\,s^{-1}$)
z	distance from upper surface of organism (m)
β	regression slope corrected for attenuation
κ_{xx}	reliability ratio
ρ	fluid density ($kg\,m^{-3}$)
σ_c	circumferential stress ($N\,m^{-2}$)
σ_l	longitudinal stress ($N\,m^{-2}$)
σ_m	muscle stress ($N\,m^{-2}$)
τ_{max}	maximum shear stress in the wall of a cylinder ($N\,m^{-2}$)

This research was supported by an NSF Graduate Research Fellowship, a University of California at Berkeley Frankhauser Fellowship and a Sigma Xi Grants-in-Aid of Research to K.Q., by NSF Grant 92-20525 to M. Koehl and R. Keller, and ONR Grant 444095-23068 to M. Koehl. I am especially grateful to M. Koehl for helpful discussion and advice, and to the members of the biomechanics group at the University of California at Berkeley for their insights and suggestions. I am grateful to M. Koehl, O. Ellers, M. Martinez and two anonymous referees for critical reading of this manuscript.

References

ADAMS, D. S., KELLER, R. AND KOEHL, M. A. R. (1990). The mechanics of notochord elongation, straightening and stiffening in the embryo of *Xenopus laevis*. *Development* **110**, 115–130.

ALEXANDER, R. MCN. (1971). *Size and Shape*. London: Edward Arnold.

ALEXANDER, R. MCN. (1983). *Animal Mechanics*. Second edition. Oxford: Blackwell Scientific Publications.

ARTHUR, D. R. (1965). Form and function in the interpretation of feeding in lumbricid worms. *Viewpoints Biol.* **4**, 204–251.

BATHAM, E. J. AND PANTIN, C. F. A. (1950). Muscular and hydrostatic action in the sea-anemone *Metridium senile*. *J. exp. Biol.* **27**, 264–289.

CALDER, W. A. (1984). *Size, Function and Life History*. Cambridge, MA: Harvard University Press.

CHAPMAN, G. (1950). On the movement of worms. *J. exp. Biol*. **27**, 29–39.

CHAPMAN, G. (1958). The hydrostatic skeleton in the invertebrates. *Biol. Rev.* **33**, 338–371.

CHAPMAN, M. A. AND NEWELL, G. E. (1947). The role of the body fluid in relation to movement in soft-bodied invertebrates. I. The burrowing of *Arenicola*. *Proc. R. Soc. Lond. B* **134**, 431–455.

CLARK, R. B. (1964). *Dynamics of Metazoan Evolution*. Oxford: Clarendon Press.

CLARK, R. B. AND COWEY, J. B. (1958). Factors controlling the change of shape of certain nemertean and turbellarian worms. *J. exp. Biol.* **35**, 731–748.

CURREY, J. D. (1970). *Animal Skeletons*. New York: St Martin Press.

DARWIN, C. (1881). *The Formation of Vegetable Mould through the Action of Worms, with Observations of their Habitats*. London: Murray.

EDWARDS, C. A. AND BOHLEN, P. J. (1996). *Biology and Ecology of Earthworms*. New York: Chapman & Hall.

ELLERS, O. AND TELFORD, M. (1992). Causes and consequences of fluctuating coelomic pressure in sea urchins. *Biol. Bull. Mar. biol. Lab., Woods Hole* **182**, 424–434.

EVANS, A. C. (1946). Distribution of number and segments in earthworms and its significance. *Nature* **158**, 98–99.

FULLER, W. A. (1987). *Measurement of Error Models*. New York: John Wiley & Sons.

GANS, C. (1973). *Biomechanics: An Approach to Vertebrate Biology*. Ann Arbor: The University of Michigan Press.

GERE, J. M. AND TIMOSHENKO, S. P. (1984). *Mechanics of Materials*. Second edition. Boston: PWS Engineering.

GOULD, S. J. (1966). Allometry and size in ontogeny and phylogeny. *Biol. Rev.* **41**, 587–640.

GRAY, J. AND LISSMANN, H. W. (1938). Studies in locomotion. VII. Locomotory reflexes in the earthworm. *J. exp. Biol.* **15**, 506–517.

HARVEY, P. H. AND PAGEL, M. D. (1991). *The Comparative Method in Comparative Biology*. Oxford: Oxford University Press.

HILL, A. V. (1950). The dimensions of animals and their muscular dynamics. *Sci. Prog.* **38**, 209–230.

HUXLEY, J. S. (1932). *Problems of Relative Growth*. London: Methuen.

JOHNSON, A. S. AND KOEHL, M. A. R. (1994). Maintenance of dynamic strain similarity and environmental stress factor in different flow habitats: thallus allometry and material properties of a giant kelp. *J. exp. Biol*. **195**, 381–410.

KIER, W. M. (1992). Hydrostatic skeletons and muscular hydrostats. In *Biomechanics (Structures and Systems): A Practical Approach* (ed. A. A. Biewener), pp. 205–231. Oxford: IRL Press.

KIER, W. M. AND SMITH, K. K. (1985). Tongues, tentacles and trunks: The biomechanics of movement in muscular hydrostats. *J. Linn. Soc.* **83**, 307–324.

LEPESCHEUX, L. (1988). Spatial organization of collagen in annelid cuticle: order and defects. *Biol. Cell* **62**, 17–31.

MCMAHON, T. (1973). Size and shape in biology. *Science* **179**, 1201–1204.

MCMAHON, T. A. (1975). Using body size to understand the structural design of animals: Quadrupedal locomotion. *J. appl. Physiol.* **39**, 619–627.

MCMAHON, T. A. AND BONNER, J. T. (1983). *On Size and Life*. New York: W. H. Freeman & Company.

NEWELL, G. E. (1950). The role of the coelomic fluid in the movements of earthworms. *J. exp. Biol.* **27**, 110–121.

PEDLEY, T. J. (1977). *Scale Effects in Animal Locomotion*. New York: Academic Press.

PETERS, R. H. (1983). *The Ecological Implications to Body Size*. Cambridge: Cambridge University Press.

PETERSON, J. A., BENSON, J. A., NGAI, M., MORIN, J. AND OW, C. (1982). Scaling in tensile 'skeletons': structures with scale-independent length dimensions. *Science* **217**, 1267–1270.

PIEARCE, T. G. (1983). Functional morphology of lumbricid earthworms, with special reference to locomotion. *J. nat. Hist.* **17**, 95–111.

RICHARDS, S. (1974). The ultrastructure of the cuticle of some British lumbricids (Annelida). *J. Zool., Lond.* **172**, 303–316.

RUBIN, C. T. AND LANYON, L. E. (1984). Dynamic strain similarity in vertebrates: an alternative to allometric limb bone scaling. *J. theor. Biol.* **107**, 321–327.

RUPPERT, E. E. AND BARNES, R. D. (1995). *Invertebrate Zoology*. Sixth edition. New York: Saunders College Publishing.

SATCHELL, J. E. (1967). Lumbricidae. In *Soil Biology* (ed. A. Burgess and F. Raw), pp. 259–322. London: Academic Press.

SCHMIDT-NIELSEN, K. (1984). *Scaling: Why is Animal Size so Important?* Cambridge: Cambridge University Press.

SEYMOUR, M. K. (1969). Locomotion and coelomic pressure in *Lumbricus terrestris* L. *J. exp. Biol.* **51**, 47–58.

SEYMOUR, M. K. (1970). Skeletons of *Lumbricus terrestris* L. and *Arenicola marina* (L.). *Nature* **228**, 383–385.

SOKAL, R. R. AND ROHLF, F. J. (1969). *Biometry*. San Francisco, CA: W. H. Freeman & Company.

STEPHENSON, J. (1930). *The Oligochaeta.* Oxford: Oxford University Press.

THOMPSON, D. W. (1917). *On Growth and Form.* Cambridge: Cambridge University Press.

TRUEMAN, E. R. (1966). Observations on the burrowing of *Arenicola marina* (L.). *J. exp. Biol.* **44**, 93–118.

TRUEMAN, E. R. (1975). *Locomotion in Soft-bodied Animals.* London: Edward Arnold.

WAINWRIGHT, S. A. (1988). *Axis and Circumference*. Cambridge, MA: Harvard University Press.

ZUCKERKANDL, E. (1988). Coelomic pressure in *Sipunculus nudus*. *Biol. Bull. mar. biol. Lab., Woods Hole* **98**, 161–173.